Research Article

Petroleum and Chemical Industry International

Seismo Electric Transfer Function Fractal Dimension for Characterizing Shajara Reservoirs Of The Permo-Carboniferous Shajara Formation, Saudi Arabia

Khalid Elyas Mohamed Elameen AlKhidir

Department of petroleum and Natural Gas Engineering, College of Engineering, King Saud University, Saudi Arabia

***Corresponding author**

Khalid Elyas Mohamed Elameen Alkhidir, Department of Petroleum and Natural Gas engineering, College of Engineering, King Saud University, Riyadh Saudi Arabia, Tel: +966114679118; E-mail: kalkhidir@ksu.edu.sa

Submitted: 27 June 2018; **Accepted**: 06 Aug 2018; **Published**: 27 Aug 2018

Abstract

The quality of a reservoir can be described in details by the application of seismo electric transfer function fractal dimension. The objective of this research is to calculate fractal dimension from the relationship among seismo electric transfer fuction, maximum seismo electric transfer function and wetting phase saturation and to confirm it by the fractal dimension derived from the relationship among capillary pressure and wetting phase saturation. In this research, porosity was measured on real collected sandstone samples and permeability was calculated theoretically from capillary pressure profile measured by mercury intrusion techniques. Two equations for calculating the fractal dimensions have been employed. The first one describes the functional relationship between wetting phase saturation, seismo electric transfer function, maximum seismo electric transfer function and fractal dimension. The second equation implies to the wetting phase saturation as a function of capillary pressure and the fractal dimension. Two procedures for obtaining the fractal dimension have been developed. The first procedure was done by plotting the logarithm of the ratio between seismo electric transfer function and maximum seismo electric transfer function versus logarithm wetting phase saturation. The slope of the first procedure = 3- Df (fractal dimension). The second procedure for obtaining the fractal dimension was completed by plotting the logarithm of capillary pressure versus the logarithm of wetting phase saturation. The slope of the second procedure = Df -3. On the basis of the obtained results of the constructed stratigraphic column and the acquired values of the fractal dimension, the sandstones of the Shajara reservoirs of the Shajara Formation were divided here into three units. The gained units from bottom to top are: Lower Shajara Seismo Electric Transfer Function Fractal Dimension Unit, Middle Shajara Seismo Electric Tranfser Function Fractal dimension Unit, and Upper Shajara Seismo Electric Transfer Function Fractal Dimension Unit. The results show similarity between seismo electric transfer tunction fractal dimension and capillary pressure fractal dimension. It was also noted that samples with wide range of pore radius were characterized by high values of fractal dimension due to an increase in their connectivity and seismo electric transfer function. In our case , and as conclusions the higher the fractal dimension, the higher the permeability, the better the shajara reservoir characteristics.

Introduction

Seismo electric effects related to electro kinetic potential, dielectric permitivity, pressure gradient, fluid viscosity, and electric conductivty was first reported by Frenkel J [1]. Capillary pressure follows the scaling law at low wetting phase saturation was reported by Li K, et al. [2]. Seismo electric phenomenon by considering electro kinetic coupling coefficient as a function of effective charge density, permeability, fluid viscosity and electric conductivity was reported by Revil A, et al. [3]. The magnitude of seismo electric current depends porosity, pore size, zeta potential of the pore surfaces, and elastic properties of the matrix was investigated by Dukhin A, et al. [4]. The tangent of the ratio of converted electic field to pressure is approximately in inverse proportion to permeability was studied by Guan W, et al. [5]. Permeability inversion from seismoelectric log at low frequency was studied by Hu H, et al. [6]. They reported that, the tangent of the ratio among electric excitation intensity and pressure field is a function of porosity, fluid viscosity, frequency, tortuosity, fluid density and Dracy permeability. A decrease of seismo electric frequencies with increasing water content was reportet by Borde C, et al. [7]. An increase of seismo electric transfer function with increasing water saturation was studied by Jardani A, et al. [8]. An increase of dynamic seismo electric transfer function with decreasing fluid conductivity was described by Holzhauer J, et al. [9]. The amplitude of seismo electric signal increases with increasing permeability which means that the seismo electric effects are directly related to the permeability and can be used to study the permeability of the reservoir was illustrated by Rong P, et al. [10]. Seismo electric coupling is frequency dependent and decreases expontialy when frequency increases was demonstrated by Djuraev U, et al. [11]. An increase of permeability with increasing pressure head and bubble pressure fractal dimension was reported by Alkhidir KEME [12]. An increase of geometric and arithmetic relaxtion time of induced polarization fractal dimension with permeability increasing was described by Alkhidir KEME [13,14,15].

Material and method

Sandstone samples were collected from the surface type section of the Permo-Carboniferous Shajara Formation, latitude 2652 17.4, longitude 43 36 18. (Figure1). Porosity was measured on collected samples using mercury intrusion Porosimetry and permeability was derived from capillary pressure data. The purpose of this paper is to obtain seismo electric transfer function fractal dimension and to confirm it by capillary pressure fractal dimension. The fractal dimension of the first procedure is determined from the positive slope of the plot of logarithm of the ratio of seismo electric transfer function to maximum seismo electric transfer functionlog(Ψ1/3/ Ψmax1/3) versus log wetting phase saturation (logs). Whereas the fractal dimension of the second procedure is determined from the negative slope of the plot of logarithm of log capillary pressure (log Pc) versus logarithm of wetting phase saturation (log Sw).

Seismo electric transfer function can be scaled as

$$S_w = \left[\frac{\psi^{\frac{1}{3}}}{\psi_{max}^{\frac{1}{3}}}\right]^{[3-Df]} \quad (1)$$

Where Sw the water saturation, ψ the seismo electric transfer function in volt.square second / square meter,ψ_{max} the maximum seismo electric transfer function in volt.square second / square meter, and Df the fractal dimension.

Equation 1 can be proofed from

$$C_S = \left[\frac{\psi}{\rho}\right] \quad (2)$$

Where C_S, the streaming potential coefficient in volt / pascal, ψ the seismo electric transfer function in volt. Square second / square meter, and ρ, the density of the fluid in kilogram / cubic meter.

The streaming potential coefficient can also be scaled as

$$C_S = \left[\frac{V}{Q}\right] \quad (3)$$

Where V the volume in cubic meter, and Q the electric charge in coulomb.

Insert equation 3 into equation 2

$$\left[\frac{V}{Q}\right] = \left[\frac{\psi}{\rho}\right] \quad (4)$$

$$\text{But, } V = \frac{4}{3} * 3.14 * r^3 \quad (5)$$

Where r the pore radius in meter

Insert equation 5 into equation 4

$$\left[\frac{4 * 3.14 * r^3}{3 * Q}\right] = \left[\frac{\psi}{\rho}\right] \quad (6)$$

The maximum pore radius r_{max} can be scaled as

$$\left[\frac{4 * 3.14 * r_{max}^3}{3 * Q}\right] = \left[\frac{\psi_{max}}{\rho}\right] \quad (7)$$

Divide equation 6 by equation 7

$$\left[\frac{\frac{4*3.14*r^3}{3*Q}}{\frac{4*3.14*r_{max}^3}{3*Q}}\right] = \left[\frac{\frac{\psi}{\rho}}{\frac{\psi_{max}}{\rho}}\right] \quad (8)$$

Equation 8 after simplification will become

$$\left[\frac{r^3}{r_{max}^3}\right] = \left[\frac{\psi}{\psi_{max}}\right] \quad (9)$$

Take the third root of equation 9

$$\sqrt[3]{\left[\frac{r^3}{r_{max}^3}\right]} = \sqrt[3]{\left[\frac{\psi}{\psi_{max}}\right]} \quad (10)$$

Equation 10 after simplification will become

$$\left[\frac{r}{r_{max}}\right] = \left[\frac{\psi^{\frac{1}{3}}}{\psi_{max}^{\frac{1}{3}}}\right] \quad (11)$$

Take the logarithm of equation 11

$$\log\left[\frac{r}{r_{max}}\right] = \log\left[\frac{\psi^{\frac{1}{3}}}{\psi_{max}^{\frac{1}{3}}}\right] \quad (12)$$

$$\text{But, } \log\left[\frac{r}{r_{max}}\right] = \frac{\log S_w}{[3 - Df]} \quad (13)$$

Insert equation 13 into equation 12

$$\frac{\log S_w}{[3 - Df]} = \log\left[\frac{\psi^{\frac{1}{3}}}{\psi_{max}^{\frac{1}{3}}}\right] \quad (14)$$

Equation 14 after log removal will become

$$S_w = \left[\frac{\psi^{\frac{1}{3}}}{\psi_{max}^{\frac{1}{3}}}\right]^{[3-Df]} \quad (15)$$

Equation 15 the proof of equation 1 which relates the water saturation, seismo electric transfer function, maximum seismo electric transfer function and the fractal dimension.

Result and discussion

Based on field observation the Shajara Reservoirs of the Permo-Carboniferous Shajara Formation were divided here into three units as described in Figure 1.These units from bottom to top are: Lower Shajara Reservoir, Middle Shajara reservoir, and Upper Shajara Reservoir. Their attained results of the seismo electric transfer function fractal dimension and capillary pressure fractal dimension are demonstrated in Table 1. Based on the accomplished results it was found that the seismo electric transfer function fractal dimension is equal to the capillary pressure fractal dimension. The maximum value of the fractal dimension was found to be 2.7872 allocated to sample SJ13 from the Upper Shajara Reservoir as confirmed in Table 1: Whereas the minimum value 2.4379 of the fractal dimension

was reported from sample SJ3 from the Lower Shajara reservoir as presented in Table1. The seismo electric transfer function fractal dimension and capillary pressure fractal dimension were observed to increase with increasing permeability as proofed in Table1 owing to the possibility of having interconnected channels

Table 1: Petrophysical model showing the three Shajara Reservoir Units with their corresponding values of seismo electric transfer function fractal dimension and capillary pressure fractal dimension

Formation	Reservoir	Sample	Porosity %	k (md)	Positive slope of the first procedure Slope=3-Df	Negative slope of the second procedure Slope=Df-3	Seismo electric transfer function fractal dimension	Capillary pressure fractal dimension
Permo-Carboniferous Shajara Formation	Upper Shajara Reservoir	SJ13	25	973	0.2128	-0.2128	2.7872	2.7872
		SJ12	28	1440	0.2141	-0.2141	2.7859	2.7859
		SJ11	36	1197	0.2414	-0.2414	2.7586	2.7586
	Middle Shajara Reservoir	SJ9	31	1394	0.2214	-0.2214	2.7786	2.7786
		SJ8	32	1344	0.2248	-0.2248	2.7752	2.7752
		SJ7	35	1472	0.2317	-0.2317	2.7683	2.7683
	Lower Shajara Reservoir	SJ4	30	176	0.3157	-0.3157	2.6843	2.6843
		SJ3	34	56	0.5621	-0.5621	2.4379	2.4379
		SJ2	35	1955	0.2252	-0.2252	2.7748	2.7748
		SJ1	29	1680	0.2141	-0.2141	2.7859	2.7859

The Lower Shajara reservoir was symbolized by six sandstone samples (Figure 1), four of which considered as SJ1, SJ2, SJ3 and SJ4 as confirmed in Table 1 were selected for capillary pressure measurement. Their positive slopes of the first procedure and negative slopes of the second procedure are defined in (Figure 2, Figure 3, Figure 4, Figure 5 and Table 1).Their seismo electric transfer function fractal dimension and capillary pressure fractal dimension values were proofed in Table 1. As we continue from sample SJ2 to SJ3 a noticeable reduction in permeability due to compaction was reported from 1955 md to 56 md which reproduces decrease in seismo electric transfer function fractal dimension and capillary pressure fractal dimension from 2.7748 to 2.4379 as quantified in Table 1. Again, an increase in grain size and permeability was noted from sample SJ4 whose seismo electric transfer function fractal dimension and capillary pressure fractal dimension was found to be 2.6843 as described in Table 1.

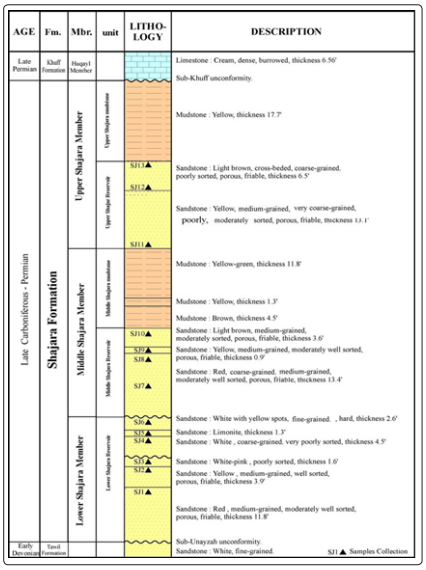

Figure 1: Surface type section of the Shajara Reservoirs of the permo-Carboniferous Shajara formation latitude 26 52 17.4 longitude 43 36 18

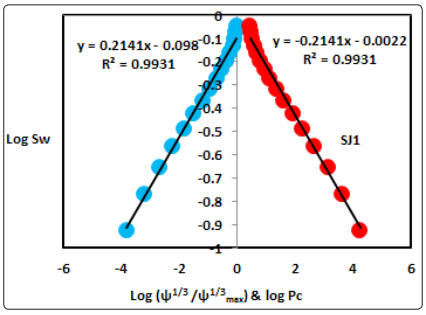

Figure 2: Log ($\Psi^{1/3}$ /$\Psi_{max}^{1/3}$) vs log Sw (blue color) & log pc vs log Sw (red color) for sample

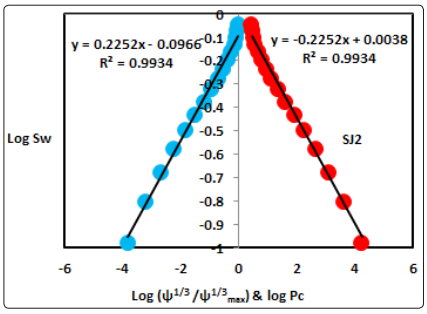

Figure 3: Log ($\Psi^{1/3}$ /$\Psi_{max}^{1/3}$) vs log Sw (blue color) & log pc vs log Sw (red color) for sample SJ2

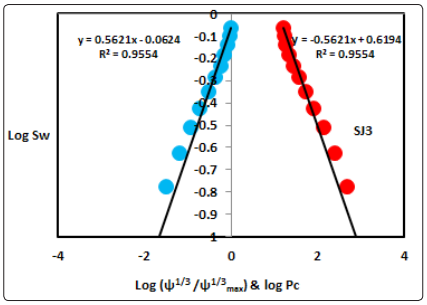

Figure 4: Log ($\Psi^{1/3}$ /$\Psi_{max}^{1/3}$) vs log Sw (blue color) & log pc vs log Sw (red color) for sample SJ3

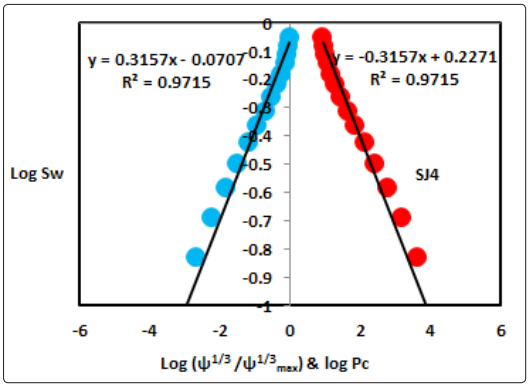

Figure 5: Log ($\Psi^{1/3}$ /$\Psi_{max}^{1/3}$) vs log Sw (blue color) & log pc vs log Sw (red color) for sample SJ4

In contrast, the Middle Shajara reservoir which is separated from the Lower Shajara reservoir by an unconformity surface as shown in Figure 1. It was designated by four samples (Fig. 1), three of which named as SJ7, SJ8, and SJ9 as illustrated in Table 1 were chosen for capillary pressure measurement.Their positive slopes of the first procedure and negative slopes of the second procedure are displayed in(Figure 6, Figure 7, Figure 8 and Table 1).Their seismo electric transfer function fractal dimensions and capillary pressure fractal dimensions show similarities as described in Table 1.Their fractal dimensions are higher than those of samples SJ3 and SJ4 from the Lower Shajara Reservoir due to an increase in their permeability as explained in Table1

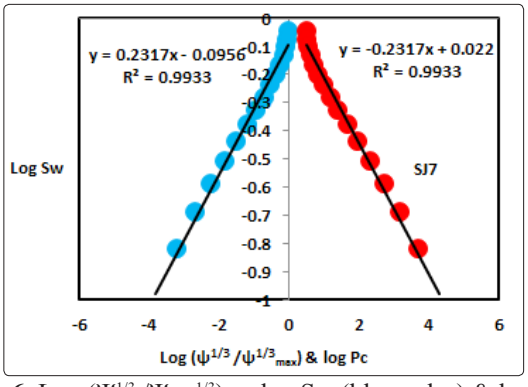

Figure 6: Log ($\Psi^{1/3}$ /$\Psi_{max}^{1/3}$) vs log Sw (blue color) & log pc vs log Sw (red color) for sample SJ7

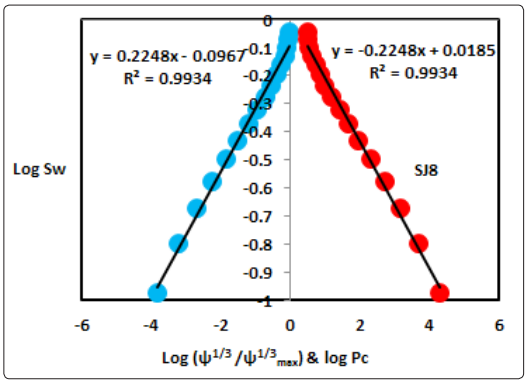

Figure 7: Log ($\Psi^{1/3}$ /$\Psi_{max}^{1/3}$) vs log Sw (blue color) & log pc vs log Sw (red color) for sample SJ8

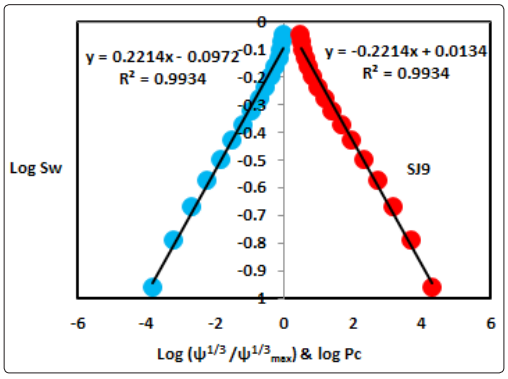

Figure 8: Log ($\Psi^{1/3}$ /$\Psi_{max}^{1/3}$) vs log Sw (blue color) & log pc vs log Sw (red color) for sample SJ9

On the other hand, the Upper Shajara reservoir is separated from the Middle Shajara reservoir by yellow green mudstone as revealed in Figure 1. It is defined by three samples so called SJ11, SJ12, SJ13 as explained in Table 1.Their positive slopes of the first procedure and negative slopes of the second procedure are displayed in (Figure 9, Figure 10, Figure 11 and Table 1).Likewise, their seismo electric transfer function fractal dimension and capillary pressure fractal dimension are also higher than those of sample SJ3 and SJ4 from the Lower Shajara Reservoir due to an increase in their permeability as explained in Table 1.

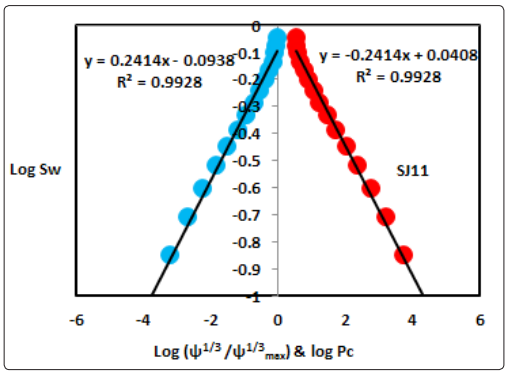

Figure 9: Log ($\Psi^{1/3}$ /$\Psi_{max}^{1/3}$) vs log Sw (blue color) & log pc vs log Sw (red color) for sample SJ11

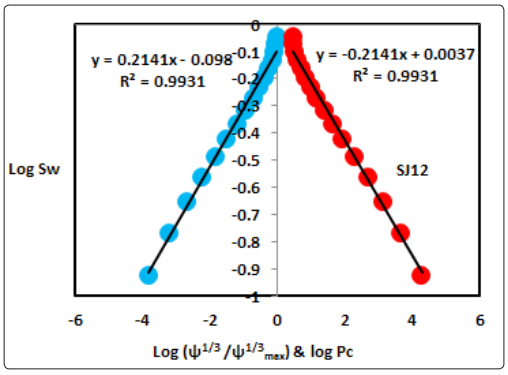

Figure 10: Log ($\Psi^{1/3}$ /$\Psi_{max}^{1/3}$) vs log Sw (blue color) & log pc vs log Sw (red color) for sample SJ12

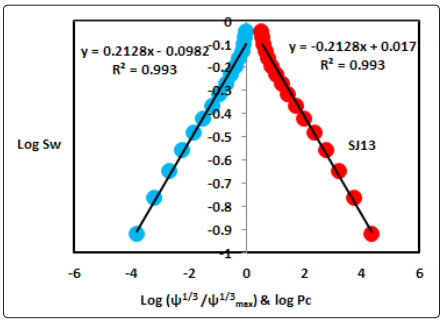

Figure 11: Log ($\Psi^{1/3}/\Psi_{max}^{1/3}$) vs log Sw (blue color) & log pc vs log Sw (red color) for sample SJ13

Inclusive a plot of seismo electric transfer function fractal dimension versus capillary pressure fractal dimension as shown in Figure 12 reveals three permeable zones of changeable Petrophysical properties. Such variation in fractal dimension can account for heterogeneity which is a key parameter in reservoir quality assessment. This heterogeneity was also shown by plotting positive slope of the first procedure versus negative slope of the second procedure as proofed in Figure 13.

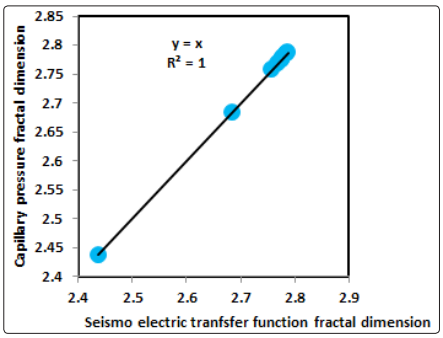

Figure 12: Seismo electric transfer function fractal dimension vs capillary pressure fractal dimension

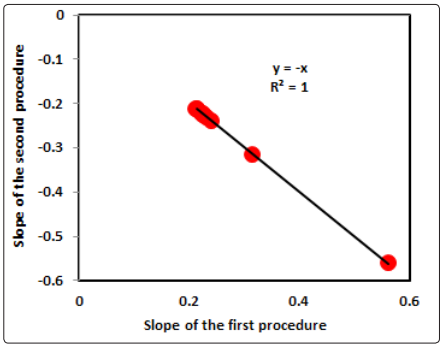

Figure 13: Slope of the first procedure vs slope of the second procedure

Conclusion

- The sandstones of the Shajara Reservoirs of thepermo-Carboniferous Shajara Formation were divided here into three units based on seismo electric transfer function fractal dimension.
- The Units from base to top are: Lower Shajara seismo electric transfer function Fractal dimension Unit, Middle Shajara seism electric transfer function Fractal Dimension Unit, and Upper Shajara seismo electric transfer function Fractal Dimension Unit.
- These units were also proved by capillary pressure fractal dimension.
- The fractal dimension was found to increase with increasing grain size and permeability.

References

1. Frenkel J (1944) On the theory of seismic and seismoelectric phenomena in a moist soil. J Physics 3: 230-241.
2. Li K, Williams W (2007) Determination of capillary pressure function from resistivity data. Transport in Porous Media 67: 1-15.
3. Revil A, Jardani A (2010) Seismoelectric response of heavy oil reservoirs: theory and numerical modelling. Geophysical J International 180: 781-797.
4. Dukhin A, Goetz P, Thommes M (2010) Seismoelectric effect: a non-isochoric streaming current. 1 experiment. J Colloid Interface Sci 345: 547-553.
5. Guan W, Hu H, Wang Z (2012) Permeability inversion from low-frequency seismoelectric logs in fluid-saturated porous formations. Geophysical Prospecting 61: 120-133.
6. Hu H, Guan W, Zhao W (2012) Theoretical studies of permeability inversion from seismoelectric logs. Geophysical Research Abstracts. 14: EGU2012-6725-1, 2012 EGU General Assembly 2012.
7. Borde C, S´en´echal P, Barri`ere J, Brito D, Normandin E, et al. (2015) Impact of water saturation on seismoel+ectric transfer functions: a laboratory study of co-seismic phenomenon. Geophysical J International 200: 1317-1335.
8. Jardani A, Revi A (2015) Seismoelectric couplings in a poroelastic material containing two immiscible fluid phases. Geophysical J International 202: 850-870.
9. Holzhauer J, Brito D, Bordes C, Brun Y, Guatarbes B (2016) Experimental quantification of the seismoelectric transfer function and its dependence on conductivity and saturation in loose sand. Geophysics Prospect 65: 1097-1120.
10. Rong P, Xing W, Rang D, Bo D, Chun L (2016) Experimental research on seismoelectric effects in sandstone. Applied Geophysics 13: 425-436.
11. Djuraev U, Jufar S, Vasant P (2017) Numerical Study of frequency-dependent seismoelectric coupling in partially-saturated porous media. MATEC Web of Conferences 87, 02001 (2017).
12. Alkhidir KEME (2017) Pressure head fractal dimension for characterizing Shajara Reservoirs of the Shajara Formation of the Permo-Casrboniferous Unayzah Group, Saudi Arabia. Archives Petroleum & Environ Biotech 2: 1-7.
13. Alkhidir KEME (2018) Geometric relaxation time of induced polarization fractal dimension for characterizing Shajara Reservoirs of the Shajara Formation of the Permo-Carboniferous Unayzah Group, Saudi Arabia. Scifed J Petroleum 2: 1-6.
14. Alkhidir KEME (2018) Geometric relaxation time of induced polarization fractal dimensionfor characterizing Shajara Reservoirs of the Shajara formation of the Permo-Carboniferous Unayzah Group-Permo. Int J Pet Res 2: 105-108.
15. Alkhidir KEME (2018) Arithmetic relaxation time of induced polarization fractal dimension for characterizing Shajara Reservoirs of the Shajara Formation. Nanosci Nanotechnol 1: 1-8.